Cell Metabolism
Article

Impaired Insulin/IGF1 Signaling Extends Life Span by Promoting Mitochondrial L-Proline Catabolism to Induce a Transient ROS Signal

Kim Zarse,[1,2] Sebastian Schmeisser,[1,3] Marco Groth,[4] Steffen Priebe,[5] Gregor Beuster,[1] Doreen Kuhlow,[1,6] Reinhard Guthke,[5] Matthias Platzer,[4] C. Ronald Kahn,[2] and Michael Ristow[1,6,*]
[1]Department of Human Nutrition, Institute of Nutrition, University of Jena, Jena D-07743, Germany
[2]Section on Integrative Physiology and Metabolism, Research Division, Joslin Diabetes Center, Harvard Medical School, Boston, MA 02215, USA
[3]Leibniz Graduate School of Aging
[4]Genome Analysis Group, Leibniz Institute for Age Research, Fritz-Lipmann-Institute, Jena D-07745, Germany
[5]Systems Biology and Bioinformatics Group, Leibniz Institute for Natural Product Research and Infection Biology, Hans-Knöll-Institute, Jena D-07745, Germany
[6]Department of Clinical Nutrition, German Institute of Human Nutrition Potsdam-Rehbrücke, Nuthetal D-14558, Germany
*Correspondence: mristow@mristow.org
DOI 10.1016/j.cmet.2012.02.013

SUMMARY

Impaired insulin and IGF-1 signaling (iIIS) in *C. elegans daf-2* mutants extends life span more than 2-fold. Constitutively, iIIS increases mitochondrial activity and reduces reactive oxygen species (ROS) levels. By contrast, acute impairment of *daf-2* in adult *C. elegans* reduces glucose uptake and transiently increases ROS. Consistent with the concept of mitohormesis, this ROS signal causes an adaptive response by inducing ROS defense enzymes (SOD, catalase), culminating in ultimately reduced ROS levels despite increased mitochondrial activity. Inhibition of this ROS signal by antioxidants reduces iIIS-mediated longevity by up to 60%. Induction of the ROS signal requires AAK-2 (AMPK), while PMK-1 (p38) and SKN-1 (NRF-2) are needed for the retrograde response. IIIS upregulates mitochondrial L-proline catabolism, and impairment of the latter impairs the life span-extending capacity of iIIS while L-proline supplementation extends *C. elegans* life span. Taken together, iIIS promotes L-proline metabolism to generate a ROS signal for the adaptive induction of endogenous stress defense to extend life span.

INTRODUCTION

In many studies on the prevention of aging, extended life span is associated with increased stress resistance. Several interventions have been described to promote both longevity and stress defense mechanisms, including calorie restriction (Weindruch and Walford, 1988; Xia et al., 1995; Masoro, 1998), physical exercise (Warburton et al., 2006; Lanza et al., 2008), and impaired insulin/IGF1 signaling (iIIS).

The eminent role of impaired IIS for the extension of life span has repeatedly been demonstrated across a wide evolutionary spectrum from nematodes (Friedman and Johnson, 1988; Kenyon et al., 1993; Morris et al., 1996; Kimura et al., 1997), to flies (Clancy et al., 2001; Tatar et al., 2001), to mice (Brown-Borg et al., 1996; Blüher et al., 2003; Holzenberger et al., 2003). These mechanisms by which impaired IIS promotes life span are not well understood but presumably involve increasing resistance against various stressors, such as thermal and oxidative stress (Vanfleteren, 1993; Vanfleteren and De Vreese, 1995; Lithgow et al., 1995; Honda and Honda, 1999; Murphy et al., 2003; Brys et al., 2010). On the other hand, impaired IIS has also been shown to increase metabolic rate and mitochondrial metabolism in both *C. elegans* (Vanfleteren and De Vreese, 1995; Houthoofd et al., 2005) and mice (Brown-Borg et al., 2012; Katic et al., 2007).

We have previously shown that reactive oxygen species (ROS) emanating from the mitochondria have an essential role for the life span-extending and health-promoting effects of glucose restriction in *C. elegans* (Schulz et al., 2007) and physical exercise in mammals (Ristow et al., 2009). In the present study, we address the hypothesis that impairment of IIS causes depletion of intracellular glucose, which is sensed by AMP-activated protein kinase (AMPK) to induce oxidative non-glucose metabolism and to generate a ROS imbalance which in turn is instrumental for the life span-extending capabilities of impaired IIS in *C. elegans*.

RESULTS

To study the effects of constitutively impaired IIS in a species-independent fashion, we have used three different models: a *C. elegans* strain carrying a mutant *daf-2(e1370)* (insulin/IGF-1 receptor homolog) gene; mouse embryonic fibroblasts (MEFs) lacking a protein primary target of both the insulin and IGF-1 receptors, namely insulin receptor substrate 1 (IRS-1) (Brüning et al., 1997) (see Figure S1A online); and lastly MEFs inducibly lacking the insulin receptor (IR) in a heterozygous fashion (previously unpublished, see the Experimental Procedures for details) (Figure S1B). These three models were independently analyzed regarding the following seven parameters.

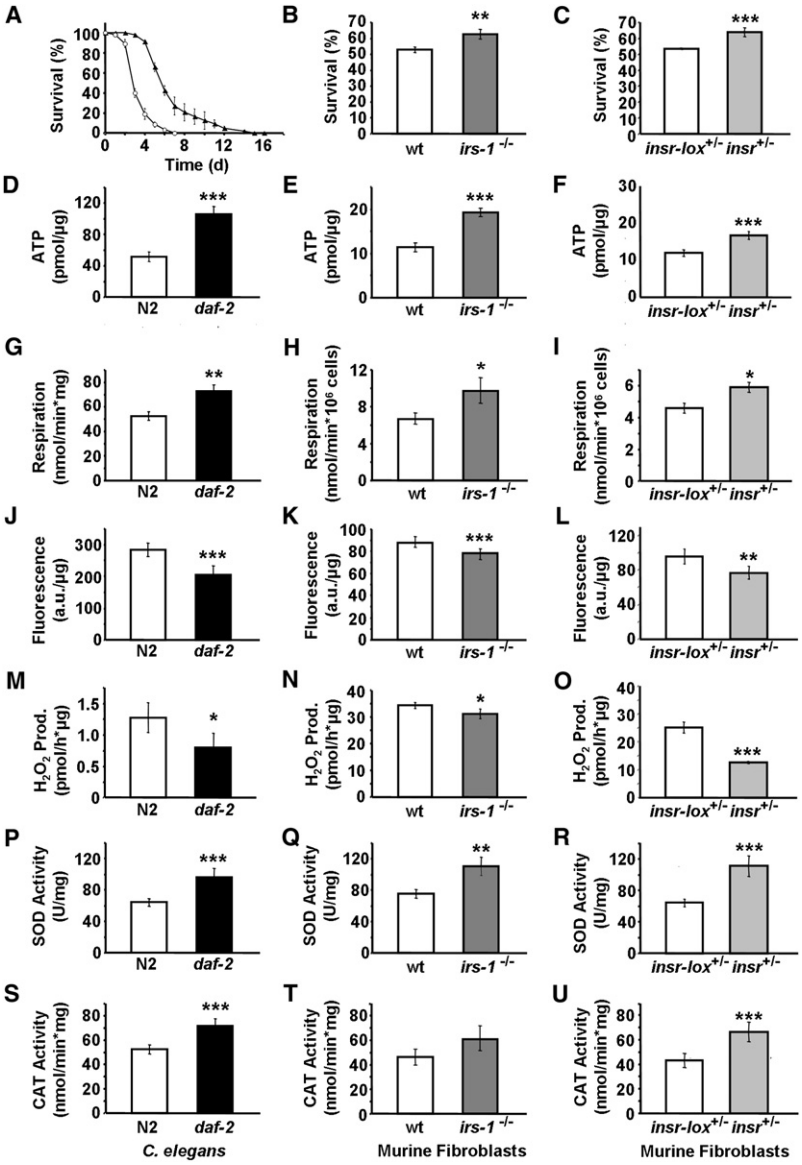

Figure 1. Constitutive Impaired Insulin-/IGF1 Signaling Induces Mitochondrial Metabolism, Reduces ROS Levels, and Increases Endogenous Antioxidant Defense in Both *C. elegans* and Murine Embryonic Fibroblasts

(A–C) Survival on paraquat, (D–F) ATP content, (G–I) oxygen consumption, (J–L) mitochondrial ROS levels, (N and O) hydrogen peroxide production, (P–R) superoxide dismutase activity, and (S–U) catalase activity, each quantified in (A, D, G, J, M, P, and S) *daf-2(e1370)* nematodes or (B, E, H, K, N, Q, and T) *irs-1*$^{-/-}$ MEFs or (C, F, I, L, O, R, and U) *insr*$^{+/-}$ MEFs (all depicted in black bars) relative to effects in the respective wild-type controls (white bars). All values are given as mean ±SD. *$p < 0.05$, **$p < 0.01$, ***$p < 0.001$ versus respective controls.

Constitutively Impaired IIS Promotes Stress Resistance

Daf-2 mutant and appropriate wild-type control strains of *C. elegans* (N2) were exposed to the established ROS generator paraquat at a concentration of 10 mM for 6 days. The *daf-2* mutant worms exhibited increased resistance against paraquat stress, as reflected by increased survival (Figure 1A) consistent with previously published data (Honda and Honda, 1999; Brys et al., 2010). Similarly, MEFs deficient for IRS1 (*irs-1*$^{-/-}$) and MEFs with heterozygous inactivation of the insulin receptor (*insr*$^{+/-}$) were more resistant to paraquat stress in vitro than control fibroblasts (Figures 1B and 1C, Figure S1C).

Constitutively Impaired IIS Increases Mitochondrial Metabolism

It has been previously suggested that impaired IIS in *C. elegans*, due to impaired expression of DAF-2, induces an increase in metabolic rate in *C. elegans* (Houthoofd et al., 2005). Indeed, in the present study we find that the ATP content in *daf-2* mutants is increased by 102% (Figure 1D). Likewise, despite the impairment in insulin/IGF-1 signaling, both *irs-1*$^{-/-}$ and *insr*$^{+/-}$ MEFs have increased ATP levels by 69% and 40%, respectively (Figures 1E and 1F), suggesting an increase in energy efficiency and mitochondrial activity in *daf-2*, *irs-1*$^{-/-}$, and *insr*$^{+/-}$. Similarly, we observed an increase in oxygen consumption by 39% of *daf-2(e1370)* mutants (Figure 1G), as well as in *irs-1*$^{-/-}$ and *insr*$^{+/-}$ by 45% and 28%, respectively (Figures 1H and 1I). Taken together, these findings indicate that chronic impairment of IIS uniformly causes an induction of mitochondrial activity in *daf-2*, *irs-1*$^{-/-}$, and *insr*$^{+/-}$.

Constitutively Impaired *daf-2* Expression Reduces ROS Levels and Induces Endogenous ROS Defense Enzymes

Mitochondria are the main source of ROS. Since impaired IIS promotes increased mitochondrial activity, as shown above (Figures 1D–1I), we anticipated that the *daf-2* mutant worms and *irs-1*$^{-/-}$ and *insr*$^{+/-}$ MEFs would exhibit increased mitochondrial ROS levels. To test this hypothesis, we have quantified ROS levels using a redox-sensitive dye that is accumulated within the mitochondrial compartment in the presence of ROS (Esposti et al., 1999). To our surprise, this revealed an unexpected reduction of ROS levels by 14%–28% in all three models (Figures 1J–1L), despite increased mitochondrial activity (Figures 1D–1I). Furthermore, when we quantified the accumulation of hydrogen peroxide in the supernatant of worms and MEFs cultures to obtain an independent estimate of ROS levels, we observed a 9%–50% reduction in all three cases (Figures 1M–1O). Thus, using two independent approaches, all three model systems of chronically impaired IIS show reduced ROS levels. Moreover, we quantified production of hydrogen peroxide in mitochondria that had been isolated from N2 and *daf-2* nematodes, respectively. Consistent with the findings in living worms (Figure 1M), we found decreased production of hydrogen peroxide in mitochondria isolated from *daf-2* mutants (Figure S1D).

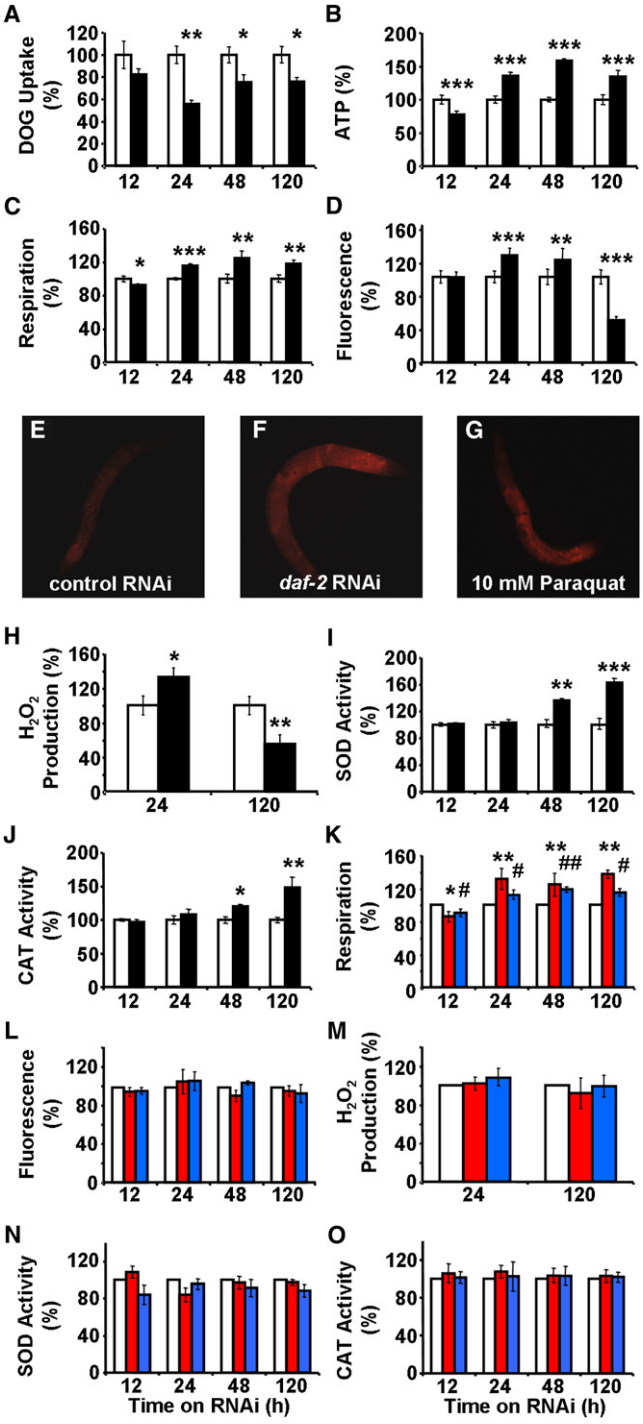

Figure 2. Acute Impairment of *daf-2* Signaling Transiently Induces Mitochondrial ROS Levels to Promote Endogenous Antioxidant Defense

(A–D) (A) 2-deoxyglucose uptake, (B) ATP content, (C) oxygen consumption, and (D) mitochondrial ROS levels each following exposure to RNAi against *daf-2* (black bars) relative to effects on control RNAi-treated nematodes (white bars) at different time points.

(E–G) Fluorescent microphotographs (enlargement, 10-fold) of MitoTracker Red CM-H_2X-treated nematodes (E) after 24 hr of control RNAi treatment, (F) after 24 hr of *daf-2* RNAi treatment, (G) after 1 hr of paraquat treatment (positive control).

(H–J) (H) Hydrogen peroxide production, (I) superoxide dismutase activity, (J) catalase activity, each following exposure to RNAi against *daf-2* (black bars) relative to effects on control RNAi-treated nematodes (white bars) at different time points.

(K–O) (K) Oxygen consumption, (L) mitochondrial ROS levels, (M) hydrogen peroxide production, (N) superoxide dismutase activity, (O) catalase activity, each following exposure to RNAi against *daf-2* in the presence of the antioxidants NAC (red bars) and BHA (blue bars) relative to effects on control RNAi-treated nematodes in the presence of antioxidants (white bars) at different time points. In all panels, relative values are depicted; for absolute values, please see Figure S2. All values are given as mean ±SD. * and $^{\#}p < 0.05$, ** and $^{\#\#}p < 0.01$, ***$p < 0.001$ versus respective controls.

To resolve how increased mitochondrial activity might be associated with decreased ROS levels, we quantified activities of antioxidant enzymes in lysates of the *C. elegans* and MEFs. Consistent with findings of others (Vanfleteren, 1993), no significant activity of glutathione peroxidase was detected in these nematodes (data not shown). However, activities of both superoxide dismutase (SOD) (Figure 1P) and catalase (CAT) (Figure 1S) were found to be increased by 50% and 36% in *daf-2* mutants, and similar findings were obtained for *irs-1*$^{-/-}$ as well as for *insr*$^{+/-}$ (Figures 1Q, 1R, 1T, and 1U). These findings indicate that in different states of chronically impaired IIS there is a decrease in ROS levels despite increased mitochondrial activity, and that this reduction is likely the result of increased activities of the major ROS defense enzymes, suggesting that the increase in ROS defense enzymes reflects an adaptive response to increased mitochondrial metabolism and possibly transiently increased ROS levels due to increased respiration.

Acutely Impaired *daf-2* Expression Causes Reduced Glucose Uptake in *C. elegans*

To test this hypothesis, we have analyzed the metabolic effects of an acute rather than constitutive *daf-2* impairment in a time-resolved manner. To this end, we administered RNAi against *daf-2*, RNAi(*daf-2*) (Dillin et al., 2002), to young adult *C. elegans* and quantified the uptake of radioactively labeled 2-deoxyglucose as a measure in insulin action. Employing this assay, we observe a persistent reduction of 2-deoxyglucose uptake in RNAi(*daf-2*)-treated nematodes by 25% (Figure 2A), consistent with long-standing evidence for reduced glucose uptake following impaired IIS in mammals.

Acutely Impaired *daf-2* Expression Activates Mitochondrial Metabolism

Reduced availability of glucose has been previously shown to activate mitochondrial metabolism in both *S. cerevisiae* (Lin et al., 2002; Barros et al., 2004) and *C. elegans* (Schulz et al., 2007). To test whether impaired DAF-2 expression would also activate mitochondrial metabolism in *C. elegans*, we performed a time course assessing metabolism after addition of RNAi(*daf-2*). Twelve hours after addition of RNAi(*daf-2*), we observed a transient reduction in respiration and ATP levels in the nematode (Figures 2B and 2C), suggesting an initial energy deficit caused by impaired glucose uptake. Consistently following this primary reduction of ATP, we observed a secondary increase in oxygen consumption which reached a maximum at 24–48 hr after addition of RNAi(*daf-2*) (Figure 2C), and this was paralleled by an increase in ATP content (Figure 2B). Taken together, these

data indicate that the nematode compensates for an energy deficit caused by decreased glucose availability by increased respiration culminating in secondarily increased ATP levels despite permanently decreased glucose uptake. The latter finding strongly suggests that energy sources other than glucose, i.e., fatty acids and/or amino acids, are likely to be metabolized.

Acutely Impaired *daf-2* Expression Promotes a Transient Increase in ROS

Increased mitochondrial activity is known to promote formation of mitochondrial ROS as an inevitable byproduct of respiration and oxidative phosphorylation. Consistent with this fact, we observed increased ROS levels 24 and 48 hr after addition of RNAi(*daf-2*) (Figures 2D–2G) when mitochondrial activity and respiration were increased. However, after 5 days of RNAi(*daf-2*) treatment, both mitochondrial activity and respiration remained increased, whereas mitochondrial ROS content was found to be significantly decreased (Figure 2D). These ROS levels were confirmed for the two key time points (24 and 120 hr) using the independent AmplexRed-based method (Figure 2H). These findings indicate that only at time points beyond 48 hr of RNAi(*daf-2*) addition, increased mitochondrial activity, as reflected by ATP content and respiration rates, is associated with a decrease in ROS levels (as reflected in the steady state, see Figure 1), whereas ROS levels are transiently increased at earlier time points.

Acutely Impaired *daf-2* Expression Secondarily Induces Endogenous ROS Defense Enzymes

To better understand the changing ROS levels, we quantified activities of antioxidant enzymes in lysates of whole nematodes. Both SOD and CAT were found to be induced following RNAi(*daf-2*) treatment for 48 and 120 hr, but interestingly not at earlier time points (Figures 2I and 2J). The relatively late induction of SOD and CAT was preceded by increases in respiration, ATP, and ROS (Figures 2B–2H). These findings suggest that adaptive inductions of both SOD and CAT activities efficiently counteract the primarily increased ROS levels culminating in decreased ROS exposure at 120 hr. We have previously observed this type of adaptive response in states of caloric restriction and physical exercise (Schulz et al., 2007; Ristow et al., 2009), while the time-resolved analysis of ROS signals preceding increased adaptive responses has not been described before.

The *daf-2*-Dependent Transient ROS Signal Is Required for Induction of Endogenous ROS Defense Enzymes

C. elegans carrying constitutively inactive alleles of *daf-2* have repeatedly been shown to be resistant to a variety of stresses (Vanfleteren, 1993; Vanfleteren and De Vreese, 1995; Lithgow et al., 1995; Honda and Honda, 1999; Murphy et al., 2003; Brys et al., 2010). Our findings of a late, i.e., secondary, induction of SOD and CAT activities following exposure of worms to RNAi(*daf-2*) suggest that transiently increased ROS levels may be required to cause this increase in ROS defense. To test this hypothesis, we have exposed RNAi(*daf-2*)-treated nematodes to two mechanistically independent antioxidants, n-acetylcysteine (NAC, 1 mM final concentration) and butylated hydroxyanisole (BHA, 25 μM final concentration). In the presence of either NAC or BHA, we still observe an induction of respiration following RNAi(*daf-2*) treatment (Figure 2K). However, both the induction of ROS levels (Figures 2L and 2M) and the secondary increase in activities of SOD and CAT (Figures 2N and 2O) were absent, indicating that increased ROS levels are required to induce endogenous ROS defense enzymes and antioxidant defense capacity. These findings indicate that RNAi(*daf-2*) is incapable of inducing SOD and CAT whenever the RNAi(*daf-2*)-mediated, transient increase in mitochondrial ROS is blocked by exogenous antioxidant supplements, even in the presence of increased respiration.

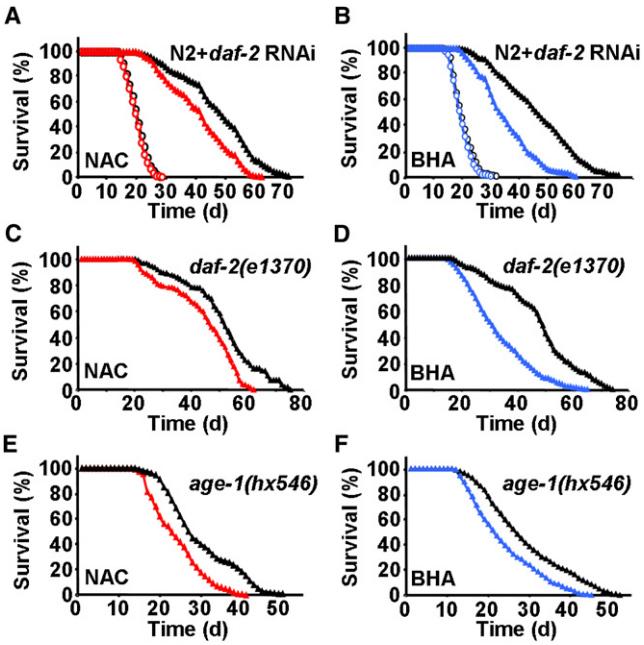

Figure 3. Exogenous Antioxidants Impair the Life Span-Extending Effects of *daf-2* and *age-1* Impairment

(A) Life span analyses of nematodes exposed to control-RNAi (open circles) in the presence (red) or absence (black) of the antioxidant NAC; life span analyses of nematodes exposed to RNAi against *daf-2* (closed triangles) in the presence (red) or absence (black) of NAC.

(B) Life span analyses in the presence of RNAi as above, replacing NAC with the antioxidant BHA (blue).

(C) Life span analyses of *daf-2(e1370)* nematodes (closed triangles) in the presence (red) or absence (black) of NAC.

(D) Life span analyses of *daf-2(e1370)* nematodes, replacing NAC with BHA (blue).

(E) Life span analyses of *age-1(hx546)* nematodes (closed triangles) in the presence (red) or absence (black) of NAC.

(F) Life span analyses of *age-1(hx546)* nematodes, replacing NAC with BHA (blue).

Exogenous Antioxidants Inhibit the Life Span-Extending Capabilities of DAF-2 and AGE-1 Deficiency

Based on these latter findings, we asked whether induction of SOD and CAT by increased ROS levels contributes to the life span-extending capabilities of impaired IIS by determining life span of NAC- or BHA-treated nematodes in the presence and absence of RNAi(*daf-2*). While no effect of antioxidants on life expectancy was observed in the absence of RNAi(*daf-2*) (Figures 3A and 3B), precluding the possibility of antioxidant toxicity on

wild-type N2 nematodes, both NAC (Figure 3A) and BHA (Figure 3B) reduced life span extension caused by RNAi(*daf-2*) treatment. As shown in more detail in Table 1, NAC impaired the life span-extending capabilities of RNAi(*daf-2*) by 35.7% (maximum life span) and 36.7% (mean life span), while BHA reduced the life span-extending capabilities of RNAi(*daf-2*) by 37.7% and 59.9% (maximum and mean life span, respectively). Moreover, NAC (Figure 3C) and BHA (Figure 3D) produced similar reduction in the long-lived worms with constitutively inactivating *daf-2(e1370)* mutation (see Table 1 for quantitative effects of antioxidants on *daf-2(e1370)* mutations). We lastly tested constitutive *age-1(hx546)* mutants which affect the *phosphoinositide-3-OH kinase* ortholog *age-1* downstream of *daf-2*, and very similarly found both NAC (Figure 3E) and BHA (Figure 3F) to reduce the life span-extending propensities of a constitutively inactivating *age-1* mutation.

These findings indicate that antioxidants reduce the life span-extending capacity produced by impaired insulin/IGF signaling in the *daf-2* and *age-1* mutants, and that a transient induction of ROS levels following impairment of *daf-2* and *age-1* signaling is required to induce an adaptive response cumulating in increased stress resistance and maximum longevity. It should be noted, however, that both RNAi(*daf-2*) exposure and the *daf-2(e1370)* as well as the *age-1(hx546)* mutations still cause a significant extension of life span in the presence of antioxidants in comparison to antioxidant-treated wild-type N2 nematodes. Altogether, this shows that exogenous antioxidants significantly lower the life span-extending capabilities of impaired IIS by up to 59.9%, whereas some other *daf-2* and *age-1* effects are independent of increased ROS levels.

The AMP-Activated Protein Kinase AAK-2 Is Essential for Induction of the Transient ROS Signal

AAK-2, the AMPK homolog, is the energy sensor in *C. elegans* (Apfeld et al., 2004; Greer et al., 2007; Schulz et al., 2007). As shown in Figure 2B, there is an initial reduction of nematodal ATP levels after addition of RNAi(*daf-2*), suggesting a reciprocal increase in nematodal AMP content. Direct assessment of AMP in *C. elegans* lysates by HPLC demonstrated an increased AMP to ATP ratio in wild-type N2 nematodes following RNAi(*daf-2*) exposure for 12 hr (AMP/ATP = +14.1% ± 6,5% SD, p = 0.038). This strongly suggests that AMP-activated AAK-2 is induced by RNAi(*daf-2*), culminating in increased mitochondrial respiration, as previously shown for states of dietary restriction (Schulz et al., 2007), and possibly here for increased ROS production.

Accordingly, we tested whether RNAi(*daf-2*) could still induce respiration and/or ROS levels in *aak-2(ok524)* mutants. However, this was not the case (Figures 4A and 4B), indicating that *aak-2* is required to generate a ROS signal in states of impaired IIS in nematodes. Nevertheless, RNAi(*daf-2*) was capable of extending life span to some extent in *aak-2(ok524)* nematodes (Figures 4C and 4D). However, it should be noted that the relative capacity of RNAi(*daf-2*) to extend life span in *aak-2(ok524)* is severely reduced compared to relative effects of RNAi(*daf-2*) on wild-type N2 (see Table 1 for quantification), indicating that a significant proportion of the effects of RNAi(*daf-2*) on life span is mediated by AAK-2 and the generation of the ROS signal as shown above (Figure 4B versus Figure 2D).

AAK-2 has been previously shown to be required for increased respiration in states of impaired glycolysis (Schulz et al., 2007). We show here that AAK-2 is also required for generating the transient ROS signal (Figure 4B). Therefore, we hypothesized that antioxidants would exert no effects on RNAi(*daf-2*)-mediated life span extension in *aak-2(ok524)* mutants, if AAK-2 is initiating the only ROS signal in the RNAi(*daf-2*)-treated worm. Indeed, both NAC (Figure 4C) and BHA (Figure 4D) had no effect on the RNAi(*daf-2*)-mediated limited extension of life span, again indicating that AAK-2 is required to generate a transient increase in ROS following RNAi(*daf-2*) treatment (see Table 1 for quantification). Taken together, these findings indicate that AAK-2 (AMPK) is an indispensable mechanistic link between impaired IIS and transiently increased ROS levels in nematodes.

The p38 MAP Kinase PMK-1 and the Transcription Factor SKN-1 (NRF-2) Are Required for Sensing of the Transient ROS Signal

Next, we questioned which pathways may be involved in ROS sensing, i.e., are required to fully exert the life span-extending effects of RNAi(*daf-2*) due to increased ROS levels. Consistent with previously published findings (Inoue et al., 2005; Schmeisser et al., 2011), we found that *pmk-1*, an ortholog of the stress-inducible mammalian *p38 MAP kinase* gene, was involved in sensing of the ROS signal generated by RNAi(*daf-2*). Thus, while RNAi(*daf-2*) caused a limited extension of life span in *pmk-1(km25)* nematodes in the absence of antioxidants (Table 1), both NAC (Figure 4E) and BHA (Figure 4F) were capable of further promoting the life span-extending capacity of RNAi(*daf-2*) (Table 1). Similar results were obtained for *skn-1(zu67)* mutants lacking a functional ortholog of the mammalian transcription factor NRF-2, which was previously shown to act downstream of PMK-1 in response to oxidative stress (Inoue et al., 2005; Tullet et al., 2008): while RNAi(*daf-2*) caused an equally limited extension of life span in *skn-1*-mutated *C. elegans* in the absence of antioxidants (Table 1), both NAC (Figure 4G) and BHA (Figure 4H) were able to further induce the life span-extending capacity of RNAi(*daf-2*) (Table 1). Consistently, the *daf-2*-mediated induction of both SOD and CAT activities (Figures 2I and 2J) was found to be reduced in nematodes constitutively deficient for PMK-1 or SKN-1 (Figures 4I and 4J), respectively.

Moreover, we have quantified differentially expressed genes in N2 wild-type nematodes in comparison to *daf-2(e1370)* mutants by applying RNA sequencing technology. Out of the genes involved in antioxidant defense, we found a number of mRNAs upregulated in *daf-2* mutants, including *sod-3* (22.6-fold, $p = 5.9 \times 10^{-88}$), *sod-5* (62.2-fold, $p = 5.7 \times 10^{-75}$), *ctl-2* (2.12-fold, $p = 1.5 \times 10^{-13}$), and *ctl-3* (1.74-fold, p = 0.00012). To test whether induction of antioxidant enzymes, and in particular *sod-3* or *ctl-2*, is necessary for the life span extension, we treated N2 nematodes with RNAi against the SOD isoform *sod-3* (Figure 4K) and the CAT isoform *ctl-2* (Figure 4L) and cotreated them with *daf-2* RNAi. We observed a reduction of life span-extending capabilities of *daf-2* RNAi in both *sod-3* and *ctl-2* RNAi-treated worms (Figures 4K and 4L) indicating that induction of antioxidant defense enzymes is, at least in part, required for the life span extension due to reduced *daf-2* signaling.

Table 1. Life Span Assay Results and Statistical Analyses

Strain, RNAi, Solvent	Maximum Life Span (d) (±SEM)	Mean Life Span (d) (±SEM)	P Value (versus Control, See Footnotes)	Number of Experiments (n)	Number of Nematodes (n)
N2 (Control RNAi) H_2O	28.0 ± 0.6	19.40 ± 0.3		3	323
N2 (Control RNAi) NAC/H_2O	27.3 ± 0.9	18.96 ± 0.2	NS[a]	3	357
N2 (*daf-2* RNAi) H_2O	70.3 ± 0.9	46.76 ± 1.0	<0.0001[a,b]	3	310
N2 (*daf-2* RNAi) NAC/H_2O	60.3 ± 0.9	39.64 ± 1.1	<0.0001[a,b,c]	3	318
N2 (Control RNAi) DMSO	31.0 ± 0.6	19.89 ± 0.2		3	335
N2 (Control RNAi) BHA/DMSO	28.3 ± 0.9	19.32 ± 0.2	NS[d]	3	331
N2 (*daf-2* RNAi) DMSO	71.7 ± 1.2	46.00 ± 1.0	<0.0001[d,e]	3	342
N2 (*daf-2* RNAi) BHA/DMSO	60.0 ± 0.6	34.16 ± 0.7	<0.0001[d,e,f]	3	331
daf-2(e1370) H_2O	73.5 ± 1.5	51.09 ± 0.6		2	218
daf-2(e1370) NAC/H_2O	61.5 ± 1.5	44.87 ± 0.5	<0.0001[g]	2	248
daf-2(e1370) DMSO	73.5 ± 1.5	47.23 ± 1.1		2	222
daf-2(e1370) BHA/DMSO	63.0 ± 2.0	31.81 ± 1.2	<0.0001[h]	2	253
age-1(hx546) H_2O	50.5 ± 0.5	28.90 ± 0.2		2	247
age-1(hx546) NAC/H_2O	41.0 ± 1.0	23.46 ± 0.2	<0.0001[i]	2	256
age-1(hx546) DMSO	50.5 ± 1.0	27,87 ± 0.2		2	259
age-1(hx546) BHA/DMSO	44.5 ± 0.5	22,63 ± 1.6	<0.0001[j]	2	242
aak-2(ok524) (Control RNAi) H_2O	24.5 ± 0.5	16.78 ± 0.4		2	213
aak-2(ok524) (Control RNAi) NAC/H_2O	24.0 ± 1.0	16.65 ± 0.3	NS[a]	2	234
aak-2(ok524) (*daf-2* RNAi) H_2O	36.0 ± 1.0	21.02 ± 0.1	<0.0001[a,b]	2	229
aak-2(ok524) (*daf-2* RNAi) NAC/H_2O	38.0 ± 1.0	21.13 ± 0.3	<0.0001[a,b], NS[c]	2	231
aak-2(ok524) (Control RNAi) DMSO	24.0 ± 1.0	16.64 ± 0.4		2	217
aak-2(ok524) (Control RNAi) BHA/DMSO	24.0 ± 0.0	16.89 ± 0.7	NS[d]	2	220
aak-2(ok524) (*daf-2* RNAi) DMSO	37.5 ± 1.5	22.53 ± 0.2	<0.0001[d,e]	2	202
aak-2(ok524) (*daf-2* RNAi) BHA/DMSO	37.5 ± 0.5	23.16 ± 0.3	<0.0001[d,e], NS[f]	2	205
pmk-1(km25) (Control RNAi) H_2O	28.0 ± 1.0	19.36 ± 0.2		2	178
pmk-1(km25) (Control RNAi) NAC/H_2O	29.5 ± 0.5	19.42 ± 0.2	NS[a]	2	160
pmk-1(km25) (*daf-2* RNAi) H_2O	38.0 ± 1.0	27.02 ± 1.1	<0.0001[a,b]	2	166
pmk-1(km25) (*daf-2* RNAi) NAC/H_2O	55.0 ± 2.0	34.13 ± 1.0	<0.0001[a,b,c]	2	170
pmk-1(km25) (Control RNAi) DMSO	26.5 ± 1.5	17.49 ± 0.7		2	157
pmk-1(km25) (Control RNAi) BHA/DMSO	28.5 ± 1.5	17.40 ± 0.6	NS[d]	2	161
pmk-1(km25) (*daf-2* RNAi) DMSO	41.5 ± 1.5	28.16 ± 1.2	<0.0001[d,e]	2	148
pmk-1(km25) (*daf-2* RNAi) BHA/DMSO	54.0 ± 2.0	32.97 ± 1.2	<0.0001[d,e], =0.00010[f]	2	151
skn-1(zu67) (Control RNAi) H_2O	21.5 ± 0.5			2	140
skn-1(zu67) (Control RNAi) NAC/H_2O	22.5 ± 0.5	16.77 ± 0.1	NS[a]	2	160
skn-1(zu67) (*daf-2* RNAi) H_2O	34.0 ± 1.0	16.57 ± 0.1	<0.0001[a,b]	2	144
skn-1(zu67) (*daf-2* RNAi) NAC/H_2O	45.5 ± 0.5	21.89 ± 0.1	<0.0001[a,b,c]	2	150
skn-1(zu67) (Control RNAi) DMSO	23.0 ± 0.0	26.71 ± 1.1		2	148
skn-1(zu67) (Control RNAi) BHA/DMSO	23.5 ± 0.5	16.78 ± 0.2	NS[d]	2	147
skn-1(zu67) (*daf-2* RNAi) DMSO	33.5 ± 1.5	16.66 ± 0.3	<0.0001[d,e]	2	158
skn-1(zu67) (*daf-2* RNAi) BHA/DMSO	45.5 ± 0.5	21.05 ± 0.3	<0.0001[d,e,f]	2	150
N2 (Control RNAi)	30.0 ± 0.5	21.0 ± 0.1		2	386
N2 (*sod-3* RNAi)	30.0 ± 1.0	20,6 ± 0.2	NS[k]	2	412
N2 (*ctl-2* RNAi)	30.0 ± 1.0	20.8 ± 0.2	NS[k]	2	452
N2 (*daf-2* RNAi)	72.0 ± 0.5	42.1 ± 1.2	<0.0001[k,l,m]	2	352
N2 (*sod-3* RNAi/*daf-2* RNAi)	55.0 ± 1.9	37.1 ± 0.7	<0.0001[k,l,n]	2	394
N2 (*ctl-2* RNAi/*daf-2* RNAi)	61.0 ± 2.4	40.1 ± 0.8	<0.05[k,m,n]	2	427
daf-16(mu86) (Control RNAi) H_2O	24.0 ± 1.0	16.71 ± 0.1		2	184
daf-16(mu86) (Control RNAi) NAC/H_2O	22.5 ± 0.5	16.35 ± 0.1	NS[a]	2	195
daf-16(mu86) (*daf-2* RNAi) H_2O	24.5 ± 0.5	16.55 ± 0.1	NS[a,b]	2	166

Table 1. *Continued*

Strain, RNAi, Solvent	Maximum Life Span (d) (±SEM)	Mean Life Span (d) (±SEM)	P Value (versus Control, See Footnotes)	Number of Experiments (n)	Number of Nematodes (n)
daf-16(mu86) (*daf-2* RNAi) NAC/H_2O	24.0 ± 0.0	16.20 ± 0.1	NS[a,b,c]	2	186
daf-16(mu86) (Control RNAi) DMSO	24.5 ± 0.5	14.68 ± 0.1		2	162
daf-16(mu86) (Control RNAi) BHA/DMSO	23.5 ± 0.5	14.62 ± 0.1	NS[d]	2	176
daf-16(mu86) (*daf-2* RNAi) DMSO	24.5 ± 0.5	14.87 ± 0.1	NS[d,e]	2	180
daf-16(mu86) (*daf-2* RNAi) BHA/DMSO	24.0 ± 0.0	14.64 ± 0.1	NS[d,e,f]	2	171
N2 (Control RNAi)	33.0 ± 0.5	22.6 ± 0.3		3	350
N2 (*B0513.5* RNAi)	32.0 ± 1.0	22.6 ± 0.1	NS[k]	2	240
N2 (*daf-2* RNAi)	69.0 ± 1.0	36.4 ± 1.9	<0.0001[k,o]	3	423
N2 (*B0513.5* RNAi/*daf-2* RNAi)	55.0 ± 1.0	31.1 ± 1.1	<0.0001[k,n,o]	3	345
N2 (H_2O)	29.5 ± 0.5	20.46 ± 0.3		2	312
L-Proline (5 μM)	33.5 ± 0.5	21.65 ± 0.1	<0.0001[p]	2	256

[a](Control RNAi) H_2O.
[b](Control RNAi) NAC/H_2O.
[c](*daf-2* RNAi) H_2O.
[d](Control RNAi) DMSO.
[e](Control RNAi) BHA/DMSO.
[f](*daf-2* RNAi) DMSO.
[g]*daf-2 (e1370)* H_2O.
[h]*daf-2 (e1370)* DMSO.
[i]*age-1(hx546)* H_2O.
[j]*age-1(hx546)* DMSO.
[k](Control RNAi).
[l](*sod-3* RNAi).
[m](*ctl-2* RNAi).
[n](*daf-2* RNAi).
[o](*B0513.5* RNAi).
[p](H_2O).

Lastly, we questioned whether *daf-16*, an ortholog of a mammalian forkhead transcription factor (FoxO), may be involved in the life span-promoting role of transiently increased ROS formation. Consistent with previously published findings, RNAi(*daf-2*) had no life span-extending effect in *daf-16(mu86)* nematodes (Figures 4M and 4N). Accordingly, neither NAC (Figure 4M) nor BHA (Figure 4N) had any detectable influence on this phenotype.

Taken together, these findings indicate that PMK-1 and SKN-1 act as transducers of the initial ROS signal following RNAi(*daf-2*) treatment to extend life span, and that this effect is mediated by transiently increased ROS levels due to the *daf-2* inactivation.

Trans-Species Transcriptome Analysis of Models of Impaired IIS

The findings depicted in Figure 1 suggest that impaired IIS causes a reduction of intracellular glucose availability which then induces mitochondrial metabolism of alternate energy substrates, i.e., fatty acids and/or amino acids, culminating in transiently increased ROS levels, as analyzed in the findings depicted in Figure 2, Figure 3, and Figure 4. To identify a potential common metabolic denominator for the ROS-dependent fraction of IIS-related life span extension, we subjected RNA samples from *daf-2* nematodes and MEFs (*irs-1*$^{-/-}$ and *insr*$^{+/-}$) to transcriptome profiling using deep sequencing (Figures 5A–5C). When analyzing those genes that were consistently either up- or downregulated in all three models, we identified three functional groups of genes (Figure 5D and Table S1). Notably, one of the upregulated groups was the MAP kinase signaling pathway (Figure 5D), strikingly consistent with the fact that disruption of the MAP kinase *pmk-1* severely impaired the effects of impaired IIS, as well as transiently increased ROS levels, as shown in Figures 4E and 4F.

Mitochondrial L-Proline Catabolism Extends Life Span in States of iIIS and Decreased Glucose Availability

By employing RNaseq, we also found that metabolism of short-chain organic acids is upregulated in states of impaired IIS. Notably, *ech-6* (encoding enoyl Coenzyme A hydratase 6)/*echs1* (encoding enoyl Coenzyme A hydratase, short chain, 1, mitochondrial), reflecting a checkpoint for catabolism of both fatty acids and amino acids, was found to be upregulated in all three models (Figure 5D and Table 2). To even better define the genes responsible for the effects of impaired IIS in a trans-species fashion, we performed a Venn analysis for all three models (Figure 5E and Table 2). Among the genes involved in the effects of impaired IIS in both mouse and worm (Table 2 and Table S1) was the orthologous pair of genes coding for a L-proline dehydrogenase (*M. musculus*, *prodh*; *C. elegans*, *B0513.5*). This enzyme is essential for catabolism of one single amino acid, L-proline, to make it available for mitochondrial oxidation and oxidative phosphorylation-based, non-glucose-based energy generation.

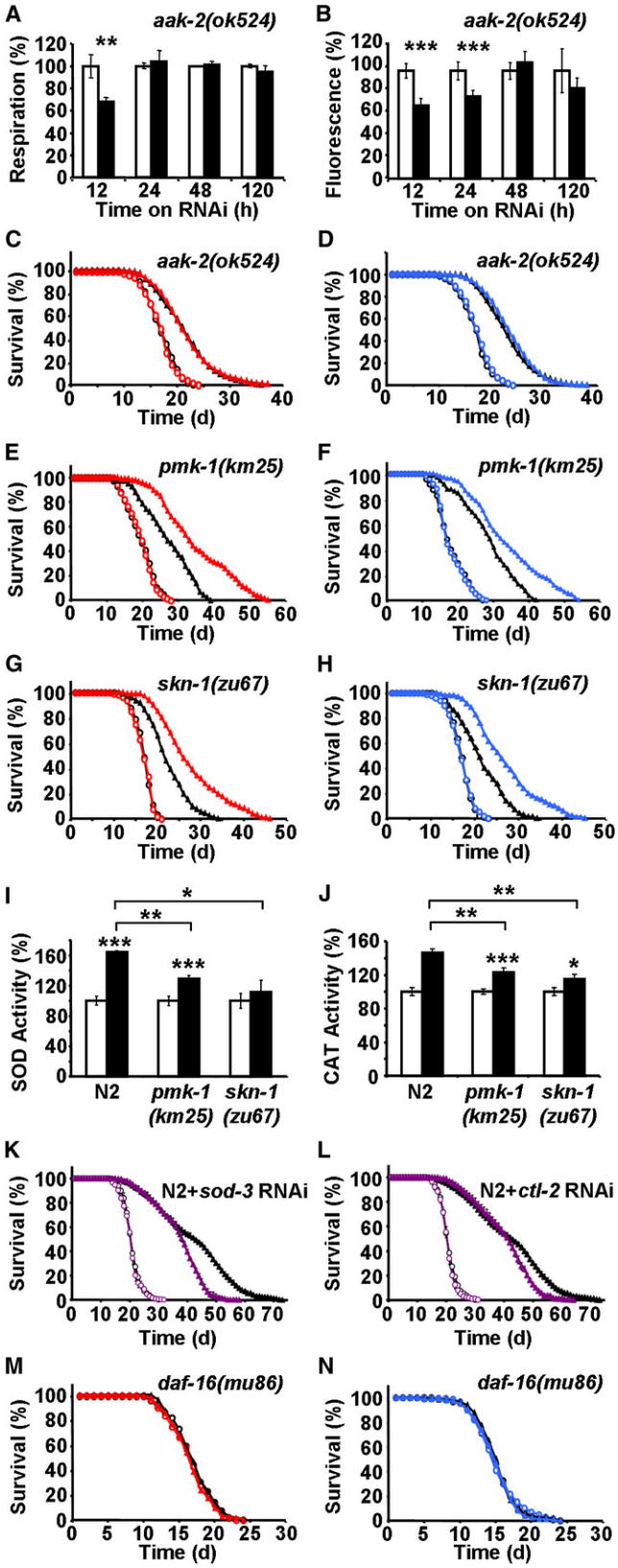

Figure 4. Molecular Regulation of ROS-Dependent Extension of Life Span Following *daf-2* Impairment

(A and B) (A) Oxygen consumption, (B) mitochondrial ROS levels in *aak2(ok524)* nematodes following exposure to RNAi against *daf-2* (black bars) relative to effects on control RNAi-treated *aak2(ok524)* nematodes (white bars) at different time points. In both panels, relative values are depicted; for absolute values, see Figure S3.

(C) Life span analyses of *aak-2(ok524)* nematodes exposed to control-RNAi (open circles) in the presence (red) or absence (black) of the antioxidant NAC; life span analyses of *aak2(ok524)* nematodes exposed to RNAi against *daf-2* (closed triangles) in the presence (red) or absence (black) of NAC.

(D) Life span analyses in the presence of mutation and RNAi as in (C), replacing NAC with the antioxidant BHA (blue).

(E) Life span analyses of *pmk-1(km25)* nematodes exposed to control-RNAi (open circles) in the presence (red) or absence (black) of NAC; life span analyses of *pmk-1(km25)* nematodes exposed to RNAi against *daf-2* (closed triangles) in the presence (red) or absence (black) of NAC.

(F) Life span analyses in the presence of mutation and RNAi as in (E), replacing NAC with BHA (blue).

(G) Life span analyses of *skn-1(zu67)* nematodes exposed to control-RNAi (open circles) in the presence (red) or absence (black) of NAC; life span analyses of *skn-1(zu67)* nematodes exposed to RNAi against *daf-2* (closed triangles) in the presence (red) or absence (black) of NAC.

(H) Life span analyses in the presence of mutation and RNAi as in (G), replacing NAC with BHA (blue).

(I and J) Activities of superoxide dismutase (I) and catalase (J) in wild-type nematodes and mutants for pmk-1 and skn-1 without (white bars) and with (black bars) *daf-2* RNAi treatment for 5 days. In (I) and (J), relative values are depicted; for absolute values, see Figure S3.

(K) Life span analyses of N2 nematodes exposed to control RNAi (empty circles) and *daf-2* RNAi (black triangles) in comparison to exposure against *sod-3* RNAi (purple circles) alone and coincubation with *daf-2* RNAi (purple triangles).

(L) Life span analyses of N2 nematodes exposed to control RNAi (empty circles) and *daf-2* RNAi (black triangles) in comparison to exposure against *ctl-2* RNAi (purple circles) alone, and coincubation with *daf-2* RNAi (purple triangles).

(M) Life span analyses of *daf-16(mu86)* nematodes exposed to control-RNAi (open circles) in the presence (red) or absence (black) of NAC; life span analyses of *daf-16(mu86)* nematodes exposed to RNAi against *daf-2* (closed triangles) in the presence (red) or absence (black) of NAC.

(N) Life span analyses in the presence of mutation and RNAi as in (M), replacing NAC with BHA (blue). In (A), (B), (I), and (J), values are given as mean ±SD. *$p < 0.05$, **$p < 0.01$, ***$p < 0.001$ versus respective controls.

To test the possibility that breakdown of L-proline may contribute to the effects of impaired IIS in a systemic manner, we treated both wild-type and *daf-2* nematodes with RNAi against *B0513.5*, the *C. elegans* ortholog of *prodh*. While knockdown of this gene has no effect on life span of N2 wild-type worms (Figure 5F), the life span-extending capability of RNAi(*daf-2*) was reduced by 14.6% and 20.3% (mean and maximum life span) following addition of RNAi(*B0513.5*) (Figure 5F).

Additionally, we have treated wild-type N2 nematodes with the amino acid L-proline in the growth media to test whether increased L-proline availability was capable of extending life span. As shown in Figure 5G, this was indeed the case, with an increase in life span by 5.8% and 13.6% (mean and maximum life span). Thus, while *B0513.5* expression is dispensable for life span in wild-type worms (Figure 5F), supplementation with L-proline can extend life span to a limited but significant extent (Figure 5G).

To additionally test whether AAK-2 (Figures 4A–4D) is responsible for the induction of L-proline metabolism in states of iIIS, we quantified expression of *B0513.5/prodh* mRNA expression in N2 as well as *aak-2* mutants in the absence

and presence of *daf-2* RNAi. Induction of *B0513.5* expression was abolished in *aak-2* mutants (Figure 5H), indicating that AAK-2 activation is located upstream of PRODH. Moreover, induction of respiration by *daf-2* RNAi (Figure 2C) was abolished by cotreatment with RNAi against *B0513.5* (Figure 5I). Likewise, RNAi against *B0513.5* abolished the ROS signal (Figure 5J) that was initially shown to be induced by *daf-2* RNAi (Figure 2D).

Together, these findings indicate that impaired IIS reduces glucose metabolism and induces L-proline catabolism in a compensatory manner to culminate in a transient ROS signal and extended life span, as summarized in Figure 5K.

DISCUSSION

We hypothesized here that reduced glucose metabolism due to impaired IIS causes a transient energy deficit and a compensatory induction of mitochondrial non-glucose metabolism to promote stress resistance and to increase longevity, both following the generation of one or several mitochondrial signaling molecules.

The findings in this study indicate that a major component, i.e., up to 59.9% of the life span extension created by reduced IIS, requires a transient increase in ROS levels. ROS then act as signaling molecules to promote life span extension. We furthermore show that this ROS signal is generated by AAK-2, an ortholog of mammalian AMPK, and is sensed by the *C. elegans* ortholog of p38 MAP kinase, PMK-1, and the ortholog of the transcription factor NRF-2, SKN-1. These sensors ultimately cause an increase in endogenous ROS defense, indicating that the ROS signal is capable of self terminating by inducing an adaptive response with increased activities of SOD and CAT, culminating in life span-extending stress resistance (Figure 5K). It is, however, likely that additional genes are activated following translocation of SKN-1, which have not been studied in the present study.

It has been proposed that ROS may act as messenger molecules in a variety of biological systems (Rhee et al., 2003; Veal et al., 2007; Finkel, 2011; Woo and Shadel, 2011). Consistently, evidence has recently emerged that ROS may also act as a life span-extending (Schulz et al., 2007; Brys et al., 2010; Pan et al., 2011) and health-promoting (Owusu-Ansah et al., 2008; Loh et al., 2009; Ristow et al., 2009) signaling molecule. This is in agreement with previous observations that calorie restriction acts by inducing low-level stress, which culminates in increased stress resistance and ultimately longevity (Xia et al., 1995; Masoro, 1998; Barros et al., 2004). In analogy to the findings presented here, this reflects a dose-dependent adaptive response commonly defined as hormesis (Southam and Ehrlich, 1943; Calabrese et al., 2007), which was later extended to the concept of mitohormesis (Tapia, 2006; Ristow and Zarse, 2010) when describing low-dose stressors emanating from the mitochondrial compartment.

The current study additionally shows for the first time that acute *daf-2* impairment reduces glucose availability in *C. elegans*, implying the fact that both glucose restriction (Schulz et al., 2007) and impaired IIS (current study) similarly cause an initial energy deficit. While some authors propose that impaired insulin/IGF-1 signaling extends life span independently of pathways activated by calorie restriction (Lakowski and Hekimi, 1998; Bartke et al., 2001; Houthoofd et al., 2003; Min et al., 2008), others have suggested that impaired IIS may share mechanistic features of caloric restriction and hence decreased energy availability, at least to some extent (Clancy et al., 2002; Al-Regaiey et al., 2005; Bonawitz et al., 2007; Greer et al., 2007; Narasimhan et al., 2009; Yen et al., 2009). Our current findings strongly support and extend this latter notion, and possibly provide a common metabolic denominator for impaired IIS, calorie restriction, and physical exercise.

In this regard, it is interesting to note that nematodes switch to mitochondrial non-glucose metabolism, as predicted in states of impaired glycolysis (Schulz et al., 2007) as well as impaired IIS (this study), by activation of AAK-2 (AMPK). Unlike for glucose, ATP generation from fatty acids and/or amino acids can only take place in the mitochondrial compartment, and requires oxidative phosphorylation. Hence, and unlike glycolysis, mitochondrial catabolism of organic acids and specifically amino acids will inevitably generate ROS which may act as signaling molecules.

One of the interesting aspects of our findings came from the combined gene expression analysis using data from three different models systems with impaired IIS, including one model in *C. elegans* and two in different murine lines. This revealed that metabolism of short-chain organic acids is upregulated in states of impaired IIS. Notably, *ech-6* (enoyl Coenzyme A hydratase 6)/*echs1* (enoyl Coenzyme A hydratase, short chain, 1, mitochondrial) reflecting a metabolic checkpoint for catabolism of both fatty acids and amino acids was found to be upregulated in all three models (Table 2 and Table S1). Moreover, and unexpectedly, a major portion of the IIS-mediated effects on life span appears to depend on a dehydrogenase, *B0513.5*, which is specifically responsible for catabolism of a single amino acid, L-proline. This is supported by the RNAi-mediated knockdown of this protein in *C. elegans* which impairs the life span-extending capabilities of impaired IIS, but does not affect life span in wild-type worms, indicating that L-proline catabolism specifically contributes to induction of mitochondrial metabolism following impairment of IIS, as shown in the current study (Figure 5K). Moreover, and—in a very general sense—somewhat consistent with our findings, increased L-proline oxidation has been linked to stress resistance in yeast (Chen et al., 2006), as well as to increased ROS formation (Donald et al., 2001) and nutrient deprivation (Pandhare et al., 2009), both in colon cancer cell lines.

Our findings on increased mitochondrial L-proline metabolism are consistent with the fact that constitutive inactivation of IIS causes increased stress resistance in *C. elegans* (Vanfleteren, 1993; Lithgow et al., 1995; Vanfleteren and De Vreese, 1995; Honda and Honda, 1999; Murphy et al., 2003; Brys et al., 2010), possibly by increasing metabolic activity (Vanfleteren and De Vreese, 1995; Houthoofd et al., 2005). This is also consistent with the finding that exogenous antioxidants, such as NAC and BHA, significantly impair the life span-extending capabilities of the constitutive *daf-2* or *age-1* mutants. This indicates that the transient increase in mitochondrial ROS observed in the current study is essential for inducing endogenous ROS defense in long-lived mutants. Similarly, in *D. melanogaster*, calorie restriction did not affect ROS production, and genetically decreased ROS production in the steady state did not extend life span in flies (Miwa et al., 2004). Consistently, altering ROS production in

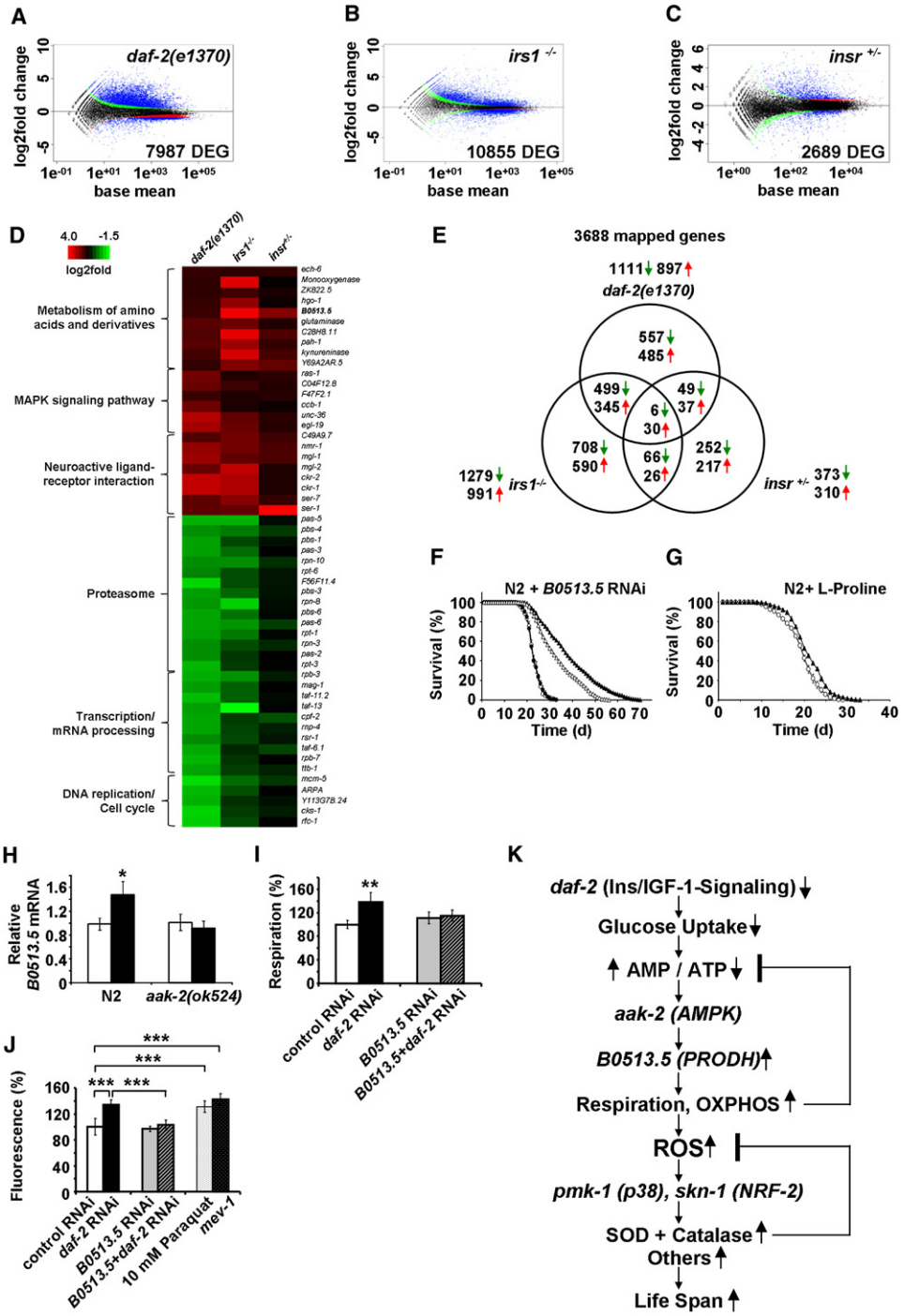

Figure 5. Trans-Species Transcriptome Analysis Identifies Increased L-Proline Catabolism as a Life Span-Extending Response to Reduced Glucose Metabolism in States of Impaired Insulin/IGF1 Signaling

(A–C) Differentially expressed genes as quantified by deep sequencing analysis for (A) *daf-2* nematodes, (B) *irs-1*$^{-/-}$ MEFs, and (C) *insr*$^{+/-}$ MEFs, all in comparison to respective controls; black dots indicate no differential regulation, red and green dots indicate regulation according to one statistical method only. Blue dots indicate regulation according to both statistical methods (used for further analysis).

(D) Functional groups of downregulated and upregulated genes (cutoff for at least two out of three sets, p = 0.05). For details, please also see Table S1.

(E) Venn analyses of differentially expressed genes derived from *daf-2* nematodes, *irs-1*$^{-/-}$ MEFs and *insr*$^{+/-}$ MEFs (cutoff for all three sets, p = 0.05). For details, please see also Table 2.

(F) Life span analyses of N2 nematodes exposed to control RNAi (empty circles) and *daf-2* RNAi (filled triangles) in comparison to exposure against *B0513.5* RNAi (closed circles) alone, and coincubation with *daf-2* RNAi (empty triangles, respectively).

(G) Life span analysis of N2 nematodes exposed to L-proline (filled triangles) or solvent (empty circles).

various model organisms has widely failed to modulate life span (Doonan et al., 2008; Jang and van Remmen, 2009; Lapointe et al., 2009; Van Raamsdonk and Hekimi, 2009). Moreover, long-lived mutants of *C. elegans* show increased stress resistance which is paralleled by increased metabolic activity (Vanfleteren and De Vreese, 1995; Houthoofd et al., 2005).

Taken together with our previous data, impaired IIS, calorie restriction, and physical exercise share, at least in part, a common metabolic denominator, i.e., activation of mitochondrial L-proline metabolism and transiently increased ROS levels, inducing an adaptive response that culminates in increased stress resistance and extends life span.

EXPERIMENTAL PROCEDURES

C. elegans Strains, Maintenance, and Life Span Assays

C. elegans strains used in this work were provided by the Caenorhabditis Genetics Center (University of Minnesota), which is supported by the NIH NCRR. Maintenance and synchronization (Lithgow et al., 1995), as well as RNAi treatments and life span assays (Dillin et al., 2002; Schulz et al., 2007), have been previously described and were performed in the absence of 5′-fluorouridine. The *B0513.5* RNAi clone was from the Ahringer library (Source BioScience, Nottingham, UK), *sod-3* and *ctl-2* RNAis were from the ORF-RNAi library (OpenBiosystems Inc., Lafayette, CO, USA), and the *daf-2* RNAi clone was a kind gift from Cynthia Kenyon (Dillin et al., 2002). NAC and BHA (both Sigma-Aldrich, St. Louis, MO, USA) were dissolved in water (NAC, 500-fold stock solution, 500 mM) and DMSO (BHA, 1,000-fold stock solution, 25 mM), respectively. Nematodes (wild-type Bristol N2 and respective mutants) were propagated on agar plates containing antioxidants or respective solvent for four generations before initiation of experiments. For L-proline (Sigma-Aldrich, St. Louis, MO, USA) supplementation experiments, the amino acid was added to autoclaved agar at 50°C as an aqueous 5 mM stock solution to obtain a final concentration of 5 μM.

Culture Conditions of *Irs-1*$^{-/-}$ MEFs

Irs-1$^{-/-}$ MEFs and control fibroblasts have been derived from two different, genetically distinct fetuses derived from the same mother as previously described (Brüning et al., 1997) and were maintained in Dulbeccos's modified Eagle's medium (DMEM) (Sigma-Aldrich, St. Louis, MO, USA) containing 10 mM D-glucose and 10% (v/v) fetal bovine serum (Biochrom AG, Berlin, Germany).

Generation and Culture Conditions of *Insr*$^{+/-}$ MEFs

Mice homozygous for the IRloxP mutation (Brüning et al., 1998) were bred with mice heterozygous for the tamoxifen-inducible Cre recombinase (CreERT2, Taconic Farms Inc., Hudson, NY, USA) [Seibler et al., 2003]), and MEFs were obtained from a single fetus that was heterozygous for both IRloxP and CreERT2. Cells then were continuously passaged and underwent crisis, all following previously described protocols (Brüning et al., 1997). Cells were then aliquoted and frozen, further serving as control fibroblasts. One aliquot of these fibroblasts was exposed to tamoxifen (Sigma-Aldrich, St. Louis, MO, USA) at a concentration of 1 μM for 7 days to obtain a heterozygous disruption of the IR. All cells were maintained and analyzed in DMEM containing 10 mM D-glucose and 10% (v/v) fetal bovine serum (Biochrom AG, Berlin, Germany). MEFs were cultured at 37°C in a humidified atmosphere of 5% CO_2.

Paraquat Stress Resistance Assay in *C. elegans*

Resistance to lethal oxidative stress derived from paraquat was determined with minor modifications as previously described (Schulz et al., 2007). Six-day (after L4)-old N2 and *daf-2(e1370)* nematodes were transferred manually to fresh NGM plates containing 10 mM paraquat (Acros Organics, Geel, Belgium) spotted with a lawn of heat-inactivated OP50 (30 min at 65°C in a water bath) followed by daily determination of the survival rate until all nematodes were dead. As described for life span analysis, worms were counted as censored in case of internal hatching, crawling off, and bursting.

Paraquat Stress Resistance Assay in Fibroblasts

One hundred thousand cells were seeded into each well of 12-well plates (TPP AG, Trasadingen, Switzerland). After 24 hr, medium was changed to DMEM containing 10 mM D-glucose and 10% (v/v) fetal bovine serum (Biochrom AG, Berlin, Germany) supplemented with 1 mM paraquat (Acros Organics, Geel, Belgium). After 48 hr, cell death was determined by propidium iodide (PI) (10 μg/ml) and Hoechst 33258 (10 μg/ml) (both Sigma-Aldrich, St. Louis, MO, USA) double fluorescent staining. Cells were examined under a fluorescence microscope (Axiovert 100, Zeiss, Oberkochen, Germany) and photographed with a digital camera (Fuji FinePix S602, Tokyo, Japan).

2-Deoxyglucose Uptake Assays

Nematodes were incubated in S-medium containing 500 μM unlabeled 2-deoxyglucose (Sigma-Aldrich, St. Louis, MO, USA) and 2.5 μCi per ml uniformly ^{14}C-labeled 2-deoxyglucose (GE Healthcare, Little Chalfont, UK), washed five times, then sonicated and centrifuged. Radioactivity in supernatant was quantified using a Beckman LS6000 liquid scintillation counter (Beckman Coulter, Brea, CA, USA). An aliquot was used for protein determination for normalization.

Determinations of ATP and AMP

Determinations of ATP and AMP were for *C. elegans*-derived samples performed by HPLC as previously described (Schulz et al., 2007) with minor modifications. For quantification of ATP content in fibroblasts, the CellTiter Glo kit (Promega, Fitchburg, WI, USA) was used according to the manufacturer's instructions, and ATP values were normalized to protein content.

Respiration Assays

Respiration assays were performed using a Clark-type electrode for *C. elegans* (Schulz et al., 2007) and mammalian cells (Ristow et al., 2000).

Mitochondrial ROS Levels

Prior to ROS measurement, MitoTracker Red CM-H_2X ROS (Invitrogen, Carlsbad, CA, USA) incubation plates were prepared as follows. For each treatment, 500 μl heat-inactivated OP50 (65°C, 30 min) was mixed with 100 μl MitoTracker Red CM-H_2X stock solution (100 μM) and spotted on a large NGM agar plate which was allowed to dry for ~1 hr. Nematodes were incubated with appropriate RNAis for time periods as indicated, then washed off the plates with S-Basal and allowed to settle by gravitation to remove offspring. Worms were washed two additional times with S-Basal and centrifuged

(H) Expression of *B0513.5/prodh* mRNA in the absence (white bars) and presence (black bars bars) of *daf-2* RNAi for 48 hr in wild-type (N2) and *aak-2* mutant nematodes.

(I) Oxygen consumption in N2 nematodes treated with control RNAi (white bars) or *daf-2* RNAi (black bars), and the additional presence of RNAi against *B0513.5/prodh* (gray/striped bars), all after 48 hr of treatment.

(J) ROS levels in nematodes treated with RNAis as in (I) for 48 hr; *mev-1(kn1)* mutants, and paraquat treatment for 1 hr serve as positive controls. In (I) and (J), relative values are depicted; for absolute values, see Figure S4. In (H)–(J), values are given as mean ±SD. *p < 0.05, **p < 0.01, ***p < 0.001 versus respective controls.

(K) Impaired insulin-/IGF1-signaling promotes L-proline catabolism to employ ROS as a mitochondrial second messenger culminating in extended life span: impaired IIS causes reduction of glucose uptake in *C. elegans*, which leads to an intermittent energy deficit that activates mitochondrial respiration by increasing L-proline catabolism in an *aak-2*-dependent manner. This induction of mitochondrial respiration generates a transient ROS signal, which is sensed by PMK-1 and SKN-1 to secondarily cause an adaptive response to increase the respective activities of superoxide dismutase and catalase which ultimately terminate the initial ROS signal, in parallel leading to increased stress resistance and extended *C. elegans* life span.

Table 2. Differentially Expressed RNAs Derived from Three Models of Impaired Insulin/IGF1 Signaling

Differentially Expressed Genes, Upregulated

C. elegans Gene	*daf-2* Log2 Fold	*daf-2* P Value	*M. Musculus* Gene	Gene Name	*irs-1*$^{-/-}$ Log2 Fold	*irs-1*$^{-/-}$ P Value	*insr*$^{+/-}$ Log2 Fold	*insr*$^{+/-}$ P Value
F25B4.8	1.629	3.012E-06	*Cenpv*	centromere protein V	2.277	8.758E-16	3.681	6.070E-15
Y71G12B.11	1.396	2.906E-11	*Tln2*	talin 2	0.438	6.274E-06	1.738	1.656E-18
bicd-1	0.710	0.0007230	*Bicd1*	bicaudal D homolog 1 (Drosophila)	1.883	3.091E-23	0.972	3.731E-05
ser-1	1.216	0.0001637	*Htr2c*	5-hydroxytryptamine (serotonin) receptor 2C	1.326	0.0008178	3.517	3.375E-19
lec-3	2.469	3.536E-26	*Lgals9*	lectin, galactose binding, soluble 9	1.593	2.012E-43	0.698	0.0009901
lec-5	2.622	1.051E-28						
lec-4	1.466	1.166E-11						
lec-1	0.776	5.248E-05						
B0513.5	**0.731**	**0.0020163**	***Prodh***	**Proline Dehydrogenase**	**3.228**	**5.120E-32**	**1.758**	**1.245E-06**
ech-6	0.650	0.0006435	*Echs1*	enoyl Coenzyme A hydratase, short chain, 1, mitochondrial	0.563	1.288E-07	0.606	0.0044002
exp-2	2.264	2.368E-12	*Kcnf1*	potassium voltage-gated channel, subfamily F, member 1	1.280	6.495E-13	0.966	0.0050530
Y55F3C.3	0.995	0.0006997						
C32C4.1	1.121	0.0016399						
F44A2.2	1.492	0.0002509						
Y48A6B.6	1.078	0.0052666						
kvs-1	0.931	0.0065899						
prk-2	1.956	1.115E-10	*Pim1*	proviral integration site 1	0.535	0.0035235	0.818	0.0015448
ras-1	1.498	2.272E-06	*Rras2*	related RAS viral (r-ras) oncogene homolog 2	0.398	4.561E-05	0.575	0.0052454
cah-2	1.365	6.083E-05	*Car10*	related RAS viral (r-ras) oncogene homolog 2	1.886	6.360E-17	1.159	0.0058154
cah-1	0.947	0.0041779						
Y73B6BL.19	2.105	8.671E-10	*Kcnd2*	potassium voltage-gated channel, Shal-related family, member 2	1.659	5.739E-08	1.186	0.0218384
C27F2.1	1.572	1.122E-05	*Wdr60*	WD repeat domain 60	1.057	2.887E-22	0.527	0.0249645
egl-3	1.162	1.113E-08	*Pcsk2*	proprotein convertase subtilisin/kexin type 2	1.478	3.103E-05	1.194	0.0296169
epac-1	2.081	6.325E-08	*Rapgef4*	Rap guanine nucleotide exchange factor (GEF) 4	0.648	0.0040905	0.877	0.0298008
exc-5	1.032	9.899E-06	*Fgd3*	FYVE, RhoGEF and PH domain containing 3	1.764	1.718E-56	0.443	0.0400597
T03G6.3	2.356	2.263E-21	*Enpp6*	ectonucleotide pyrophosphatase/phosphodiesterase 6	1.473	0.0001826	1.316	0.0482077
F47F2.1	0.727	0.0091527	*Prkx*	protein kinase, X-linked	0.372	0.0038382	0.454	0.0373704
ceh-31	2.777	1.650E-09	*Barhl2*	BarH-like 2 (*Drosophila*)	Inf	0.0201619	Inf	0.0469553
ceh-30	1.530	8.221E-05						
tub-2	0.428	0.0269801	*Tulp4*	similar to mKIAA1397 protein; tubby like protein 4	0.2171	0.0137626	0.410	0.0445156

Differentially Expressed Genes, Downregulated

C. elegans Gene	*daf-2* Log2 Fold	*daf-2* P Value	*M. Musculus* Gene	Gene Name	*irs-1*$^{-/-}$ Log2 Fold	*irs-1*$^{-/-}$ P Value	*insr*$^{+/-}$ Log2 Fold	*insr*$^{+/-}$ P Value
nuc-1	−1.880	2.085E-11	*Dnase2a*	Dnase2a deoxyribonuclease II alpha	−0.581	0.0006621	−0.643	0.0181585
F35G2.1	−0.758	0.0243548	*Qsox1*	quiescin Q6 sulfhydryl oxidase 1	−0.323	0.0091651	−0.851	0.0002569
M01F1.9	−0.911	0.0050494	*Rgp1*	RGP1 retrograde golgi transport homolog (S. cerevisiae)	−0.366	0.0035610	−0.567	0.0262451
C01B10.9	−0.696	0.0435967	*Enpp4*	ectonucleotide pyrophosphatase/phosphodiesterase 4	−1.539	8.893E-17	−2.300	8.870E-20

Table 2. *Continued*

Differentially Expressed Genes, Downregulated								
C. elegans Gene	*daf-2* Log2 Fold	*daf-2* P Value	*M. Musculus* Gene	Gene Name	*irs-1*$^{-/-}$ Log2 Fold	*irs-1*$^{-/-}$ P Value	*insr*$^{+/-}$ Log2 Fold	*insr*$^{+/-}$ P Value
T13C2.4	−1.075	0.0006532	*Ssu72*	Ssu72 RNA polymerase II CTD phosphatase homolog (yeast)	−0.515	0.0000335	−0.521	0.0430715
F53F10.3	−0.716	0.0367228	*Brp44*	brain protein 44	−0.633	0.0000076	−0.604	0.0313828

Cutoff for all three sets, p = 0.05.

(300 g, 30 s). The worm pellet was transferred to freshly prepared MitoTracker Red CM-H2X and incubated for 2 hr at 20°C. To remove excessive dye from the gut, worms were transferred to NGM agar plates with appropriate RNAis or as a positive control, to plates containing 10 mM paraquat for an additional 1 hr at 20°C. Aliquots of 100 μl worm suspension were distributed into a 96-well FLUOTRAC plate (Greiner Bio-One, Frickenhausen, Germany). Fluorescence intensity was measured in a microplate reader (FLUOstar Optima, BMG Labtech, Offenburg, Germany) using well-scanning mode (ex, 570 nm; em, 610 nm). To normalize fluorescence signal, remaining worm suspension was used for protein determination. For measuring mitochondrial ROS levels in fibroblasts, 10,000 cells were seeded into each well of a 96-well plate. After 24 hr, cells were incubated with medium containing 1 μM MitoTracker Red CM-H_2X ROS for 30 min. Cells were then washed two times with PBS, and fluorescence intensity was measured at the same conditions described above.

Amplex Red-Based Quantification of Supernatant Hydrogen Peroxide in *C. elegans*

Worms were removed from plates with 0.05 M sodium-phosphate buffer (pH 7.4), washed twice, and transferred into an upright plexiglas cylinder (1.5 ml volume) with continuous stirring at low speed (100 rpm) at 20°C. First determination of fluorescence was done without horseradish peroxidase (HRP) (Sigma-Aldrich, St. Louis, MO, USA) only in the presence of 1 μM Amplex Red (Invitrogen, Carlsbad, CA, USA) to detect possible a nonspecific increase in fluorescence (which was not observed). Next, 0.01 U/ml HRP was added, and changes of fluorescence were recorded with a fluorescence detector (LF402 ProLine, IOM, Berlin, Germany) for at least 15 min at excitation and emission wavelengths of 571 and 585 nm, respectively. Immediately afterwards, worms were removed and collected for protein determination to normalize fluorescence values. For determination of hydrogen peroxide production in fibroblasts, 10,000 cells were seeded into each well of a 96-well plate. After 24 hr, Amplex Red Assay was performed according to the manufacturer's instructions. Fluorescence intensity was measured in a microplate reader (FLUOstar Optima, BMG Labtech, Offenburg, Germany) using well-scanning mode (ex, 570 nm; em, 590 nm).

Isolation of Mitochondria

Isolation of mitochondria was performed as previously described (Kayser et al., 2001), except the initial rupture of nematodes was done by a Potter/Elvehjem tissue grinder at 400 rpm with three slow up-and-down strokes. Isolated mitochondria (50 μg) were transferred into an upright plexiglas cylinder (1.5 ml volume) with continuous stirring at low speed (100 rpm) at 30°C. Measurement of fluorescence increase due to Amplex Red oxidation was carried out as described above (for whole worms), while only 0.1 U/ml horseradish peroxidase was used. Pyruvate (2.5 mM) and 1.25 mM malate (final concentrations) were added simultaneously as substrates for the respiratory chain.

Antioxidant Enzyme Activities

Antioxidant enzyme activities (SOD, CAT) in both nematodes and MEFs were determined by standard photometric assays as previously described (Schulz et al., 2007) with minor modifications.

Fluorescent Microscopy

Worms were treated with MitoTracker Red CM-H_2X ROS exactly as described above. Individual worms were placed on agarose pads and paralyzed with 1 mg/ml tetramisole (Sigma-Aldrich, St. Louis, MO, USA). Worms were examined under a fluorescence microscope (Axiovert 100, Zeiss, Oberkochen, Germany) using the filter set (BP546/12, FT580, LP590), and pictures were taken with a digital camera (Moticam 2300, Motic, Xiamen, P.R. of China).

Protein Content

Protein content in both nematodes and MEFs was determined by standard methods as previously described (Schulz et al., 2007) with minor modifications.

Extraction of Total RNA from *C. elegans* and Fibroblasts

RNA isolation was performed using a commercially available kit (QIAGEN, Hilden, Germany, Rneasy Mini Kit) based on the phenol-chloroform extraction method according to the manufacturer's instructions.

Real-Time PCR

Reverse transcription and quantitative real-time PCR was carried out using the GoTaq 2-Step RT-qPCR System (Promega, Madison, WI, USA) according to the manufacturer's instructions on LightCycler 480 system (Roche, Mannheim, Germany). Data were normalized to cdc-42 (Hoogewijs et al., 2008) and analyzed using the $\Delta\Delta C_T$ method. Primer sequences used for B0513.3 and cdc-42 are fwd 5′-AAGCCAGCGGCGATGACACC and rev 5′-AACACCCT GCCGCCGATCTC as well as fwd 5′-CTGCTGGACAGGAAGATTACG and rev 5′-CTCGGACATTCTCGAATGAAG.

Transcriptome Profiling Using Deep Sequencing

For library preparation, 5 μg of total RNA per sample was processed using Illumina's mRNA-Seq sample prep kit (Illumina, San Diego, CA, USA) following the manufacturer's instructions. The libraries were sequenced using an Illumina GAIIx, in a single 76 nt read approach. Each library sequenced on a single lane ended up with around 30–40 mio reads per sample. Sequence data were extracted in FastQ format and used for mapping. Reads which passed the quality filtering were mapped against the *C. elegans* genome and an exon junction splice database using Bowtie (Langmead et al., 2009). Only uniquely mapped reads were used for counting. The RefSeq annotation was used to assign mapping positions to exons, transcripts, and genes. The data discussed in this publication have been deposited in NCBI's Gene Expression Omnibus and are accessible through GEO Series accession number GSE36041 (http://www.ncbi.nlm.nih.gov/geo/query/acc.cgi?acc=GSE36041).

Bioinformatics of RNA Expression Data

Raw counts for the transcripts were analyzed using the R Statistical Computing Environment (R Development Core Team, 2008) and the Bioconductor packages DESeq (Anders and Huber, 2010) and edgeR (Robinson et al., 2010). Both packages provide statistical routines for determining differential expression in digital gene expression data using a model based on the negative binomial distribution. The resulting p values were adjusted using the Benjamini and Hochberg approach for controlling the false discovery rate (FDR) (Benjamini and Hochberg, 1995). Transcripts with an adjusted p value smaller than 0.01 found by both packages (intersection) were assigned as differentially expressed.

Statistical Analyses

Data are expressed as means ±SD unless otherwise indicated. Statistical analyses for all data except life span and stress resistance assays in *C. elegans* were performed by Student's t test (unpaired, two-tailed) after testing for equal distribution of the data and equal variances within the data set. For comparing significant distributions between different groups in the life span assays and

stress resistance assays, statistical calculations were carried out using the log rank test. All calculations were performed using Excel 2007 (Microsoft, Albuquerque, NM, USA) and SPSS version 13.0 (IBM, Armonk, NY, USA). A p value below 0.05 was considered as statistically significant.

SUPPLEMENTAL INFORMATION

Supplemental Information includes four figures and one table and can be found with this article online at doi:10.1016/j.cmet.2012.02.013.

ACKNOWLEDGMENTS

C. elegans strains used in this work were provided by the Caenorhabditis Genetics Center (University of Minnesota), which is funded by the National Institutes of Health (NIH) National Center for Research Resources (NCRR). The authors thank Cynthia Kenyon for the RNAi construct against *daf-2* (Dillin et al., 2002). The excellent technical assistance of Ivonne Heinze, Beate Laube, Annett Müller, and Waltraud Scheiding, as well as the excellent secretarial assistance of Mandy Schalowski, is gratefully acknowledged. This work is part of the research program of the Jena Centre for Systems Biology of Ageing (JenAge) funded by the German Ministry for Education and Research (Bundesministerium für Bildung und Forschung; support code BMBF 0315581), and has been additionally funded by NIH grants DK31036 and DK33201 to C.R.K. Funding for this project was denied by the German Research Association (Deutsche Forschungsgemeinschaft, DFG), grant application number RI 1976/3-1.

Received: September 15, 2011
Revised: February 1, 2012
Accepted: February 23, 2012
Published online: April 3, 2012

REFERENCES

Al-Regaiey, K.A., Masternak, M.M., Bonkowski, M., Sun, L., and Bartke, A. (2005). Long-lived growth hormone receptor knockout mice: interaction of reduced insulin-like growth factor i/insulin signaling and caloric restriction. Endocrinology *146*, 851–860.

Anders, S., and Huber, W. (2010). Differential expression analysis for sequence count data. Genome Biol. *11*, R106.

Apfeld, J., O'Connor, G., McDonagh, T., DiStefano, P.S., and Curtis, R. (2004). The AMP-activated protein kinase aak-2 links energy levels and insulin-like signals to lifespan in *C. elegans*. Genes Dev. *18*, 3004–3009.

Barros, M.H., Bandy, B., Tahara, E.B., and Kowaltowski, A.J. (2004). Higher respiratory activity decreases mitochondrial reactive oxygen release and increases life span in Saccharomyces cerevisiae. J. Biol. Chem. *279*, 49883–49888.

Bartke, A., Wright, J.C., Mattison, J.A., Ingram, D.K., Miller, R.A., and Roth, G.S. (2001). Extending the lifespan of long-lived mice. Nature *414*, 412.

Benjamini, Y., and Hochberg, Y. (1995). Controlling the false discovery rate: a practical and powerful approach to multiple testing. J. R. Stat. Soc., B *57*, 289–300.

Blüher, M., Kahn, B.B., and Kahn, C.R. (2003). Extended longevity in mice lacking the insulin receptor in adipose tissue. Science *299*, 572–574.

Bonawitz, N.D., Chatenay-Lapointe, M., Pan, Y., and Shadel, G.S. (2007). Reduced TOR signaling extends chronological life span via increased respiration and upregulation of mitochondrial gene expression. Cell Metab. *5*, 265–277.

Brown-Borg, H.M., Borg, K.E., Meliska, C.J., and Bartke, A. (1996). Dwarf mice and the ageing process. Nature *384*, 33.

Brown-Borg, H.M., Johnson, W.T., and Rakoczy, S.G. (2012). Expression of oxidative phosphorylation components in mitochondria of long-living Ames dwarf mice. Age (Dordr.) *34*, 43–57.

Brüning, J.C., Winnay, J., Cheatham, B., and Kahn, C.R. (1997). Differential signaling by insulin receptor substrate 1 (IRS-1) and IRS-2 in IRS-1-deficient cells. Mol. Cell. Biol. *17*, 1513–1521.

Brüning, J.C., Michael, M.D., Winnay, J.N., Hayashi, T., Hörsch, D., Accili, D., Goodyear, L.J., and Kahn, C.R. (1998). A muscle-specific insulin receptor knockout exhibits features of the metabolic syndrome of NIDDM without altering glucose tolerance. Mol. Cell *2*, 559–569.

Brys, K., Castelein, N., Matthijssens, F., Vanfleteren, J.R., and Braeckman, B.P. (2010). Disruption of insulin signalling preserves bioenergetic competence of mitochondria in ageing Caenorhabditis elegans. BMC Biol. *8*, 91.

Calabrese, E.J., Bachmann, K.A., Bailer, A.J., Bolger, P.M., Borak, J., Cai, L., Cedergreen, N., Cherian, M.G., Chiueh, C.C., Clarkson, T.W., et al. (2007). Biological stress response terminology: integrating the concepts of adaptive response and preconditioning stress within a hormetic dose-response framework. Toxicol. Appl. Pharmacol. *222*, 122–128.

Chen, C., Wanduragala, S., Becker, D.F., and Dickman, M.B. (2006). Tomato QM-like protein protects Saccharomyces cerevisiae cells against oxidative stress by regulating intracellular proline levels. Appl. Environ. Microbiol. *72*, 4001–4006.

Clancy, D.J., Gems, D., Harshman, L.G., Oldham, S., Stocker, H., Hafen, E., Leevers, S.J., and Partridge, L. (2001). Extension of life-span by loss of CHICO, a Drosophila insulin receptor substrate protein. Science *292*, 104–106.

Clancy, D.J., Gems, D., Hafen, E., Leevers, S.J., and Partridge, L. (2002). Dietary restriction in long-lived dwarf flies. Science *296*, 319.

Dillin, A., Crawford, D.K., and Kenyon, C. (2002). Timing requirements for insulin/IGF-1 signaling in C. elegans. Science *298*, 830–834.

Donald, S.P., Sun, X.Y., Hu, C.A., Yu, J., Mei, J.M., Valle, D., and Phang, J.M. (2001). Proline oxidase, encoded by p53-induced gene-6, catalyzes the generation of proline-dependent reactive oxygen species. Cancer Res. *61*, 1810–1815.

Doonan, R., McElwee, J.J., Matthijssens, F., Walker, G.A., Houthoofd, K., Back, P., Matscheski, A., Vanfleteren, J.R., and Gems, D. (2008). Against the oxidative damage theory of aging: superoxide dismutases protect against oxidative stress but have little or no effect on life span in Caenorhabditis elegans. Genes Dev. *22*, 3236–3241.

Esposti, M.D., Hatzinisiriou, I., McLennan, H., and Ralph, S. (1999). Bcl-2 and mitochondrial oxygen radicals. New approaches with reactive oxygen species-sensitive probes. J. Biol. Chem. *274*, 29831–29837.

Finkel, T. (2011). Signal transduction by reactive oxygen species. J. Cell Biol. *194*, 7–15.

Friedman, D.B., and Johnson, T.E. (1988). A mutation in the age-1 gene in Caenorhabditis elegans lengthens life and reduces hermaphrodite fertility. Genetics *118*, 75–86.

Greer, E.L., Dowlatshahi, D., Banko, M.R., Villen, J., Hoang, K., Blanchard, D., Gygi, S.P., and Brunet, A. (2007). An AMPK-FOXO pathway mediates longevity induced by a novel method of dietary restriction in *C. elegans*. Curr. Biol. *17*, 1646–1656.

Holzenberger, M., Dupont, J., Ducos, B., Leneuve, P., Geloen, A., Even, P.C., Cervera, P., and Le Bouc, Y. (2003). IGF-1 receptor regulates lifespan and resistance to oxidative stress in mice. Nature *421*, 182–187.

Honda, Y., and Honda, S. (1999). The daf-2 gene network for longevity regulates oxidative stress resistance and Mn-superoxide dismutase gene expression in Caenorhabditis elegans. FASEB J. *13*, 1385–1393.

Hoogewijs, D., Houthoofd, K., Matthijssens, F., Vandesompele, J., and Vanfleteren, J.R. (2008). Selection and validation of a set of reliable reference genes for quantitative sod gene expression analysis in C. elegans. BMC Mol. Biol. *9*, 9.

Houthoofd, K., Braeckman, B.P., Johnson, T.E., and Vanfleteren, J.R. (2003). Life extension via dietary restriction is independent of the Ins/IGF-1 signalling pathway in Caenorhabditis elegans. Exp. Gerontol. *38*, 947–954.

Houthoofd, K., Fidalgo, M.A., Hoogewijs, D., Braeckman, B.P., Lenaerts, I., Brys, K., Matthijssens, F., De Vreese, A., Van Eygen, S., Munoz, M.J., and Vanfleteren, J.R. (2005). Metabolism, physiology and stress defense in three aging Ins/IGF-1 mutants of the nematode Caenorhabditis elegans. Aging Cell *4*, 87–95.

Inoue, H., Hisamoto, N., An, J.H., Oliveira, R.P., Nishida, E., Blackwell, T.K., and Matsumoto, K. (2005). The C. elegans p38 MAPK pathway regulates nuclear localization of the transcription factor SKN-1 in oxidative stress response. Genes Dev. *19*, 2278–2283.

Jang, Y.C., and van Remmen, H. (2009). The mitochondrial theory of aging: Insight from transgenic and knockout mouse models. Exp. Gerontol. *44*, 256–260.

Katic, M., Kennedy, A.R., Leykin, I., Norris, A., McGettrick, A., Gesta, S., Russell, S.J., Bluher, M., Maratos-Flier, E., and Kahn, C.R. (2007). Mitochondrial gene expression and increased oxidative metabolism: role in increased lifespan of fat-specific insulin receptor knock-out mice. Aging Cell *6*, 827–839.

Kayser, E.B., Morgan, P.G., Hoppel, C.L., and Sedensky, M.M. (2001). Mitochondrial expression and function of GAS-1 in Caenorhabditis elegans. J. Biol. Chem. *276*, 20551–20558.

Kenyon, C., Chang, J., Gensch, E., Rudner, A., and Tabtiang, R. (1993). A C. elegans mutant that lives twice as long as wild type. Nature *366*, 461–464.

Kimura, K.D., Tissenbaum, H.A., Liu, Y., and Ruvkun, G. (1997). daf-2, an insulin receptor-like gene that regulates longevity and diapause in Caenorhabditis elegans. Science *277*, 942–946.

Lakowski, B., and Hekimi, S. (1998). The genetics of caloric restriction in Caenorhabditis elegans. Proc. Natl. Acad. Sci. USA *95*, 13091–13096.

Langmead, B., Trapnell, C., Pop, M., and Salzberg, S.L. (2009). Ultrafast and memory-efficient alignment of short DNA sequences to the human genome. Genome Biol. *10*, R25.

Lanza, I.R., Short, D.K., Short, K.R., Raghavakaimal, S., Basu, R., Joyner, M.J., McConnell, J.P., and Nair, K.S. (2008). Endurance exercise as a countermeasure for aging. Diabetes *57*, 2933–2942.

Lapointe, J., Stepanyan, Z., Bigras, E., and Hekimi, S. (2009). Reversal of the mitochondrial phenotype and slow development of oxidative biomarkers of aging in long-lived Mclk1+/− mice. J. Biol. Chem. *284*, 20364–20374.

Lin, S.J., Kaeberlein, M., Andalis, A.A., Sturtz, L.A., Defossez, P.A., Culotta, V.C., Fink, G.R., and Guarente, L. (2002). Calorie restriction extends Saccharomyces cerevisiae lifespan by increasing respiration. Nature *418*, 344–348.

Lithgow, G.J., White, T.M., Melov, S., and Johnson, T.E. (1995). Thermotolerance and extended life-span conferred by single-gene mutations and induced by thermal stress. Proc. Natl. Acad. Sci. USA *92*, 7540–7544.

Loh, K., Deng, H., Fukushima, A., Cai, X., Boivin, B., Galic, S., Bruce, C., Shields, B.J., Skiba, B., Ooms, L.M., et al. (2009). Reactive oxygen species enhance insulin sensitivity. Cell Metab. *10*, 260–272.

Masoro, E.J. (1998). Hormesis and the antiaging action of dietary restriction. Exp. Gerontol. *33*, 61–66.

Min, K.J., Yamamoto, R., Buch, S., Pankratz, M., and Tatar, M. (2008). Drosophila lifespan control by dietary restriction independent of insulin-like signaling. Aging Cell *7*, 199–206.

Miwa, S., Riyahi, K., Partridge, L., and Brand, M.D. (2004). Lack of correlation between mitochondrial reactive oxygen species production and life span in Drosophila. Ann. N Y Acad. Sci. *1019*, 388–391.

Morris, J.Z., Tissenbaum, H.A., and Ruvkun, G. (1996). A phosphatidylinositol-3-OH kinase family member regulating longevity and diapause in Caenorhabditis elegans. Nature *382*, 536–539.

Murphy, C.T., McCarroll, S.A., Bargmann, C.I., Fraser, A., Kamath, R.S., Ahringer, J., Li, H., and Kenyon, C. (2003). Genes that act downstream of DAF-16 to influence the lifespan of Caenorhabditis elegans. Nature *424*, 277–283.

Narasimhan, S.D., Yen, K., and Tissenbaum, H.A. (2009). Converging pathways in lifespan regulation. Curr. Biol. *19*, R657–R666.

Owusu-Ansah, E., Yavari, A., Mandal, S., and Banerjee, U. (2008). Distinct mitochondrial retrograde signals control the G1-S cell cycle checkpoint. Nat. Genet. *40*, 356–361.

Pan, Y., Schroeder, E.A., Ocampo, A., Barrientos, A., and Shadel, G.S. (2011). Regulation of yeast chronological life span by TORC1 via adaptive mitochondrial ROS signaling. Cell Metab. *13*, 668–678.

Pandhare, J., Donald, S.P., Cooper, S.K., and Phang, J.M. (2009). Regulation and function of proline oxidase under nutrient stress. J. Cell. Biochem. *107*, 759–768.

R Development Core Team. (2008). R: A Language and Environment for Statistical Computing (Vienna, Austria: Foundation for Statistical Computing).

Rhee, S.G., Chang, T.S., Bae, Y.S., Lee, S.R., and Kang, S.W. (2003). Cellular regulation by hydrogen peroxide. J. Am. Soc. Nephrol. *14*, S211–S215.

Ristow, M., and Zarse, K. (2010). How increased oxidative stress promotes longevity and metabolic health: the concept of mitochondrial hormesis (mitohormesis). Exp. Gerontol. *45*, 410–418.

Ristow, M., Pfister, M.F., Yee, A.J., Schubert, M., Michael, L., Zhang, C.Y., Ueki, K., Michael, M.D., 2nd, Lowell, B.B., and Kahn, C.R. (2000). Frataxin activates mitochondrial energy conversion and oxidative phosphorylation. Proc. Natl. Acad. Sci. USA *97*, 12239–12243.

Ristow, M., Zarse, K., Oberbach, A., Klöting, N., Birringer, M., Kiehntopf, M., Stumvoll, M., Kahn, C.R., and Blüher, M. (2009). Antioxidants prevent health-promoting effects of physical exercise in humans. Proc. Natl. Acad. Sci. USA *106*, 8665–8670.

Robinson, M.D., McCarthy, D.J., and Smyth, G.K. (2010). edgeR: a Bioconductor package for differential expression analysis of digital gene expression data. Bioinformatics *26*, 139–140.

Schmeisser, S., Zarse, K., and Ristow, M. (2011). Lonidamine extends lifespan of adult Caenorhabditis elegans by increasing the formation of mitochondrial reactive oxygen species. Horm. Metab. Res. *43*, 687–692.

Schulz, T.J., Zarse, K., Voigt, A., Urban, N., Birringer, M., and Ristow, M. (2007). Glucose restriction extends *Caenorhabditis elegans* life span by inducing mitochondrial respiration and increasing oxidative stress. Cell Metab. *6*, 280–293.

Seibler, J., Zevnik, B., Kuter-Luks, B., Andreas, S., Kern, H., Hennek, T., Rode, A., Heimann, C., Faust, N., Kauselmann, G., et al. (2003). Rapid generation of inducible mouse mutants. Nucleic Acids Res. *31*, e12.

Southam, C.M., and Ehrlich, J. (1943). Effects of extract of western red-cedar heartwood on certain wood-decaying fungi in culture. Phytopathology *33*, 517–524.

Tapia, P.C. (2006). Sublethal mitochondrial stress with an attendant stoichiometric augmentation of reactive oxygen species may precipitate many of the beneficial alterations in cellular physiology produced by caloric restriction, intermittent fasting, exercise and dietary phytonutrients: 'Mitohormesis' for health and vitality. Med. Hypotheses *66*, 832–843.

Tatar, M., Kopelman, A., Epstein, D., Tu, M.P., Yin, C.M., and Garofalo, R.S. (2001). A mutant Drosophila insulin receptor homolog that extends life-span and impairs neuroendocrine function. Science *292*, 107–110.

Tullet, J.M., Hertweck, M., An, J.H., Baker, J., Hwang, J.Y., Liu, S., Oliveira, R.P., Baumeister, R., and Blackwell, T.K. (2008). Direct inhibition of the longevity-promoting factor SKN-1 by insulin-like signaling in *C. elegans*. Cell *132*, 1025–1038.

Vanfleteren, J.R. (1993). Oxidative stress and ageing in Caenorhabditis elegans. Biochem. J. *292*, 605–608.

Vanfleteren, J.R., and De Vreese, A. (1995). The gerontogenes age-1 and daf-2 determine metabolic rate potential in aging Caenorhabditis elegans. FASEB J. *9*, 1355–1361.

Van Raamsdonk, J.M., and Hekimi, S. (2009). Deletion of the mitochondrial superoxide dismutase sod-2 extends lifespan in Caenorhabditis elegans. PLoS Genet. *5*, e1000361. 10.1371/journal.pgen.1000361.

Veal, E.A., Day, A.M., and Morgan, B.A. (2007). Hydrogen peroxide sensing and signaling. Mol. Cell *26*, 1–14.

Warburton, D.E., Nicol, C.W., and Bredin, S.S. (2006). Health benefits of physical activity: the evidence. CMAJ *174*, 801–809.

Weindruch, R., and Walford, R.L. (1988). The Retardation of Aging and Disease by Dietary Restriction (Springfield, Ill: Charles C Thomas Pub Ltd).

Woo, D.K., and Shadel, G.S. (2011). Mitochondrial stress signals revise an old aging theory. Cell *144*, 11–12.

Xia, E., Rao, G., Van Remmen, H., Heydari, A.R., and Richardson, A. (1995). Activities of antioxidant enzymes in various tissues of male Fischer 344 rats are altered by food restriction. J. Nutr. *125*, 195–201.

Yen, K., Patel, H.B., Lublin, A.L., and Mobbs, C.V. (2009). SOD isoforms play no role in lifespan in ad lib or dietary restricted conditions, but mutational inactivation of SOD-1 reduces life extension by cold. Mech. Ageing Dev. *130*, 173–178.